Cai *et al. Advances in Bridge Engineering* (2023) 4:15
https://doi.org/10.1186/s43251-023-00093-2

Advances in
Bridge Engineering

ORIGINAL INNOVATION Open Access

Research on the mechanism of an adaptive device to deal with bridgehead jump

Bingliang Cai[1], Deyi Chen[1*] and Shiping Huang[2,3]

*Correspondence:
dychen@yangtzeu.edu.cn

[1] School of Urban Construction, Yangtze University, Jingzhou 434000, China
[2] School of Civil Engineering and Transportation, South China University of Technology, Guangzhou 510640, China
[3] China-Singapore International Joint Research Institute, Guangzhou 510700, China

Abstract

This article aims to solve the problem of the vehicle bumping at bridgehead which caused by uneven settlement in the transition section of the road and bridge. Firstly, a new adaptive device was established. In addition, the mechanism of the device was revealed. Secondly, analytical calculations were performed for the hitch plate equipped with the adaptive device, the deflection equation was derived, and the analytical solution was compared with the numerical solution. Finally, the adaptive device was applied to the actual project, the elongation of the device was analyzed with the settlement of the hitch plate. The results show that the adaptive device can realize the smooth transition of the road-bridge connection section by self-adjustment. Thus, the bridge head jump can be avoided in the case of soil foundation settlement, overall settlement and slap slope. The analytical and numerical solutions of the maximum deflection at the end of the slab are 2.571 cm and 2.263 cm. The corresponding longitudinal slope change rates are 2.8‰ and 2.5‰. One year after the completion of the actual project, the elongation of the two devices is 1.63 cm and 1.97 cm, and the settlement of the end of the slap is 3.74 cm. The adaptive device can provide a reference for solving the problem of jumping traffic at the bridge head.

Keywords: Bridge engineering, Bumping at bridgehead, Adaptive device, Analytical solution, Numerical simulation

1 Introduction

With the increase of highway mileage and bridge construction in China, bridge head jumping has become a common issue in the field of bridge engineering. Due to the existence of settlement differences in the transition section of the road and bridge, when vehicles drive through, strong bumps may occur, which can easily lead to traffic safety accidents. The impact load imposed by the vehicle on the road intensify the slap and bridge damage, increase the road maintenance costs; In addition, the uneven settlement caused by the violent bumps reduce the service life of the vehicle, affecting the comfort of the occupants. At present, it is often used to set the bridge head lap, geogrid, etc. as a solution to the bridge head jump, and has achieved some success. However, the laps are susceptible to fracture under impact loading when in a soft foundation situation.

Establishing an accurate load-induced settlement model is a key issue in calculating the response of bridgehead jump. In terms of theoretical design, Wang et al. (2015)

analyzed the differential settlement of foundations, the centrifugal test was used to observe differential settlements in different position between foundations on the basis of investigation. The research results show that both in horizontal and vertical directions, evident differential settlement exists in a limited area on both sides of the vertical interface between different foundations. In order to study the influence of uneven foundation settlement on the seismic performance of a structure, Bao et al. (2019) used the incremental dynamic analysis (IDA) method to analyze the seismic vulnerability of the steel structure frame. Sharma et al. (2009) proposed a failure mechanism for reinforced soil foundations based on the results of the literature review and the experimental study of model foundations conducted by the authors. Then, based on the proposed failure mechanisms, new bearing capacity equations were developed for reinforced sandy and silty clay foundations, which include the contribution of the reinforcement to the increase in bearing capacity.

In terms of dealing with the bridge head jumping problem, Chen and Abu-Farsakh (2016) proposed a new design for the approach slab, which requires increasing the slab flexural rigidity (El), and using reinforced soil foundation (RSF) to support the slab and traffic loads at the roadway pavement/approach slab joint (R/S joint). Liu et al. (2022) investigated the differential settlement of the road-bridge transition section exacerbated by the periodic movement of abutments caused by seasonal temperature changes. In this study, three physical tests were designed and conducted to fill this knowledge gap. For performing the analysis, Chakraborty and Kumar (2014) separately considered three different soil media, namely, (i) fully granular, (ii) cohesive frictional, and (iii) fully cohesive with an additional provision to account for an increase of cohesion with depth. The results have been obtained (i) for different values of phi in case of fully granular ($c=0$) and c-phi soils, and (ii) for different rates (m) at which the cohesion increases with depth for a purely cohesive soil (phi = 0 degrees). Long et al. (1998) studied differential motion at the structural interface of road embankments-bridges in Illinois. Research shows that the sources of differential movement in Illinois can be divided into six major categories: (a) compression or erosion of materials at the approach ernbankment-abutment interface, (b) a broken approach slab, (c) compression of foundation soils, (d) compression or internal erosion of embankment soils, (e) poor construction grade control, and (f) areal distortion of foundation soils. Briaud and Lim (1997) studied the deformation characteristics of soil nail wall at the back of bridge abutment by finite element model. Lin and Wong (1999) used a composite foundation with variable length cement mixing piles to deal with the bridge head jump problem. It is concluded that the variable length cement mixing pile is easy and efficient to deal with the differential settlement in the transition section of road and bridge. After a lot of research and practice by domestic and foreign scholars, the measures to deal with bridge head jumping have been improved and given more reasonable solutions in engineering practice.

In improving the design and application of slaps, Wong (1994) conducted an experimental study on the secondary jumping problem at the end of the lap slab due to the damage and sinking of the lap slab at the bridge head. He proposed that the concrete lap slab at the bridge head should be made at a certain slope, and the thickness of the corresponding pavement layer should be adjusted according to the change of the slope. Yasrobi et al. (2016) conducted a study on the operation of the hitch in twelve states in

the U.S. and found that when the longitudinal slope difference of the hitch in the transition section of the road and bridge reaches 0.6% to 1.0%, the hitch structure will be damaged more severely and passengers will feel discomfort on board. Chen and Abu-Farsakh (2015) used the reinforced soil foundation(RSFs) to increase the soil bearing capacity and to reduce the potential footing settlement. New bearing capacity formulas, which consider both the confinetnent and the membrane effects of reinforcements on the increase in ultimate bearing capacity, were then developed for strip footings on RSFs. With the continuous development of bridge head slap in simulation, experiment and design, the technology of slap as the treatment of uneven settlement of road and bridge is gradually improved, which provides theoretical support to solve the problem of bridge head jumping.

The above studies provide valuable explorations from different perspectives for evaluating the slap treatment of bridgehead jump. However, few studies have applied dynamic support to bridge head slap to solve the jumping problem. Its mechanism needs to be further studied. In view of the existing problems, this paper firstly proposes an adaptive device to prevent and control the bridge head jumping, and proposes a specific solution for the settlement at each position of the hitch plate in view of the deficiencies of the existing technology. Secondly, the feasibility of the adaptive device is verified by combining the analytical and numerical solutions. Finally, the adaptive device is applied to the actual project, and the elongation and the settlement at the end of the hitch plate of the two devices are compared and analyzed.

2 Introduction to adaptive devices and their mechanism of action

2.1 Introduction to the device

Adaptive device for the prevention of bridge head jumps, comprising a first hitch plate, a second hitch plate, a pile base, a hydraulic device, a telescopic sleeve, a mirror-reflective photoelectric switch, a horizontal switch and a contact switch. The first slap is set below the road surface layer, one end is fixed to the bridge deck by means of reinforcement and the other end is placed on the roadbed by means of a mat; the second slap is set at a certain depth below the road surface layer; the hydraulic device is fixed at two or three points of the second slap and the pile is set below the second slap as a supporting structure; the mirror-reflective photoelectric switch transmitter is fixed at the side of the bridge, see Fig. 1.

Among them, 31 is a telescopic casing, providing telescoping effect when the equipment is running; 32, 34 is an insulated wooden board, acting as a fixed shell; 33 is an insulated shell, when the device is tilted, the circuit is closed and the switch is opened to start the device for adjustment. 35 is a horizontal switch, influenced by the shell 33. 36 is a contact switch, directly controlling the switching and closing of the circuit. 51 for the photoelectric switch transmitter, 52 for the special reflector, the two form a mirror-reflective photoelectric switch to control the start of the device. 331 for the wire, 332 for the mercury, 333 for the groove, the three form a mercury control device, the insulation device to control the start of the telescopic casing. 37 for the brake, when the device is finished telescoping, the brake is activated to control the hydraulic device no longer rise.

Compared with the prior art, the beneficial effect of the technical solution proposed by this new device is that by controlling the hydraulic device, the structure as a whole

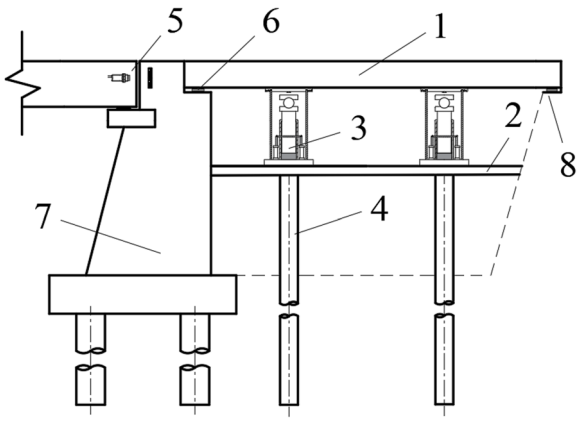

Fig. 1 Overall view of the abutment and adaptive device

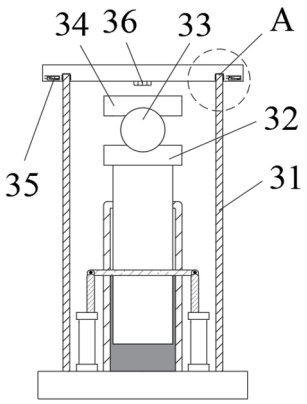

Fig. 2 Hydraulic device diagram

adapts to the problems of possible overall settlement, tilting of the first hitch plate and settlement of the soil behind the platform, saving the cost of later manual repair and maintenance, and effectively improving the problem of jumping of the bridge head caused by poor settlement.

2.2 Specific implementation

Referring to Figs. 1 and 2, the ends of the first hitch 1 are placed on the abutment 7 and the roadbed 8 provided with pads 6, the second hitch 2 is fixed to the abutment 7 by means of a reinforcement at one end and extends into the soil base at the other end, the lower part of the hydraulic unit 3 is fixed to the second hitch 2 by means of a pallet.

Referring to Figs. 2 and 3, the upper part of the telescopic sleeve 31 is provided with a projection 311, which is combined with a recess 312 set in the upper pallets of the device and leaves a gap.

Referring to Figs. 2 and 3, the horizontal switch 35 is externally a sealed insulated housing with about one-fifth of mercury 332 inside. When a tilt occurs and reaches a certain angle, the mercury 332 will flow to the lower part of the container due to gravity, and if it touches both electrodes at the same time, the circuit will close and the switch will open.

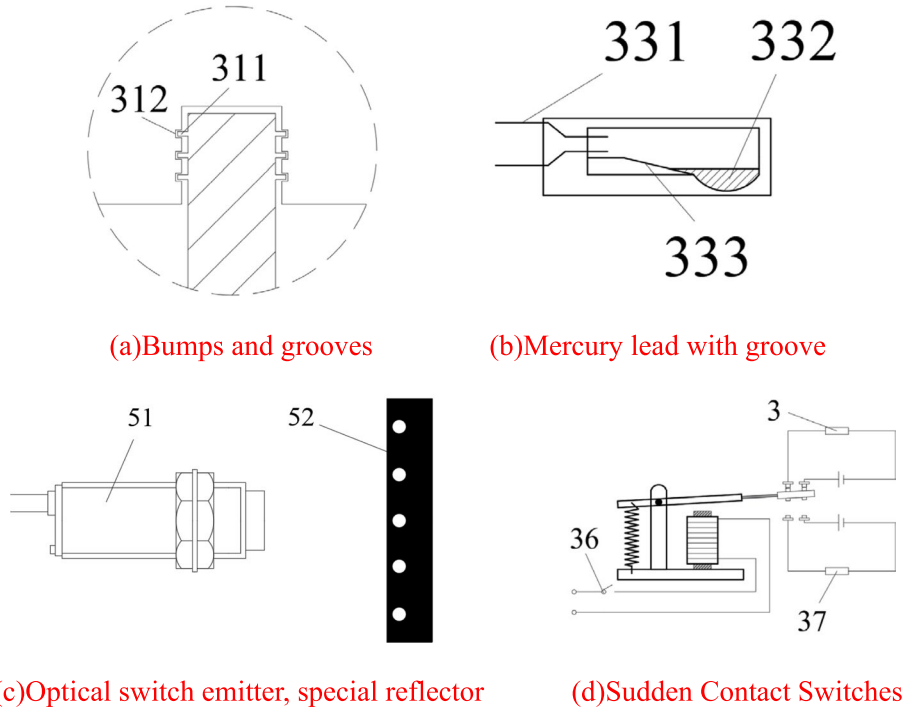

Fig. 3 Detail construction drawing

Referring to Figs. 1 and 3, the mirror-reflective photoelectric switch 5 is composed of a photoelectric switch transmitter 51 and a special reflector 52. Among them, mirror-reflective photoelectric switch 5 two parts of the axis in the same horizontal line, but the special reflector 52 width to be greater than the photoelectric switch emitter 51 to receive the reflection of the range.

2.3 Mechanism of action

Referring to Figs. 2 and 3, when the soil base behind the abutment 7 settles, the expansion sleeve 31 becomes longer to accommodate the settlement, the second inner concave plate separates from the contact switch 36, the power supply is disconnected and the hydraulic device 3 is activated, when it rises to contact with the contact switch 36, the power supply is closed, the brake 37 is activated, the hydraulic device 3 no longer rises and fixes the current position so that the first hitch plate 1 remains at the same height as the bridge deck, thus making the first hitch plate 1 consistent with the bridge deck. avoid triggering the bridge to jump.

Referring to Figs. 1 and 3, when the overall settlement is produced, the photoelectric switch emitter 51 can not receive the light beam reflected by the special reflector 52, the power supply is disconnected and the hydraulic device 3 starts, when the rise to the photoelectric switch emitter 51 can receive the light beam reflected by the special reflector 52, the power supply is closed, the brake 37 starts, the hydraulic device 3 no longer rises and fixes the current position, thus making the first hitch plate 1 and the bridge deck maintain the same height, avoiding triggering the bridge jump. Mirror reflective photoelectric switch 5 circuit principle is the same as the contact switch 36.

Referring to Figs. 2 and 3, when the first hitch plate 1 is tilted, the mercury 332 contacts the two wires 331, the switch closes and the hydraulic device 3 starts, when it rises until the mercury 332 is separated from the wires 331, the power supply breaks, the brake 37 starts, the hydraulic device 3 no longer rises and fixes the current position. This allows the first hitch 1 to remain smoothly connected to the bridge deck, avoiding triggering a jump at the bridge. The horizontal switch 35 circuit principle is similar to the contact switch 36, the difference is that the hydraulic device 3 and the brake 37 are in the opposite circuit.

In summary, this device can self-adapt to a variety of situations in practice by setting the first hitch plate 1, second hitch plate 2, pile base 4, hydraulic device 3, mirror-reflective photoelectric switch 5, horizontal switch 35 and contact switch 36. By self-adjusting and thus avoiding the phenomenon of bridge head jumping, it solves the current problems of imperfect bridge head jumping prevention and control measures, poor self-adaptive ability and high maintenance cost in the later stage.

3 Analytical solutions for deflection

3.1 Basic assumptions

To investigate the static characteristics of the adaptive device, the device was simplified to a flexible foundation beam with a fixed left end and a free right end, with a vertical uniform load above the beam and a hinged support at each of the three points below the beam to limit upward and downward movement, as shown in Fig. 4.

Basic assumptions: Foundation beams are of finite length and have a flexibility index $\beta l < \pi$. Where $\beta = \sqrt[4]{\frac{kb}{EI}}$ is the characteristic value of the flexibility of the beam, k is the coefficient of elasticity of the foundation, b is the width of the beam and EI is the flexural stiffness of the beam section.

3.2 Derivation of the deflection equation

For any finite length section of an elastic foundation beam, the deflection equation for the unloaded section is expressed by the initial parameter method Briaud and Lim (1997) as

$$y = y0 \bullet \phi 1 + \theta 0 \frac{\phi 2}{\beta} - M0 \frac{\phi 3}{EI\beta^2} - Q0 \frac{\phi 4}{EI\beta^3} \tag{1}$$

where $y0$, $\theta 0$, $M0$, $Q0$ is the deflection, angle of rotation, bending moment and shear force at the end point of the finite length beam, i.e. the initial parameters, and $\phi 1$, $\phi 2$, $\phi 3$, $\phi 4$ is the Krylov function with respect to βl.

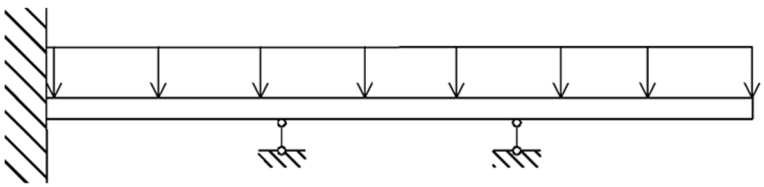

Fig. 4 Mechanically simplified analytical model

$$\begin{aligned}\phi 1 &= ch\beta x\cos\beta x\\ \phi 2 &= \frac{1}{2}(ch\beta x\sin\beta x + sh\beta x\cos\beta x)\\ \phi 3 &= \frac{1}{2}sh\beta x\sin\beta x\\ \phi 4 &= \frac{1}{4}(ch\beta x\sin\beta x - sh\beta x\cos\beta x)\end{aligned} \tag{2}$$

The upper part of the foundation beam is subjected to a uniform load q, the lower part of the beam is an adaptive device at two trilaterals, which are reduced to vertical supports, and the two support reactions $P1 = \frac{22}{63}ql, P2 = \frac{4}{7}ql$ are obtained by the force method. in this case, the foundation beam is subjected to a uniform load above and a concentrated load below, and the deflection equation requires the addition of the deflection correction term.

When $x \in [0, \frac{l}{3}]$, the correction term is $q\frac{1-\phi 1(\beta x)}{k}$

When $x \in (\frac{l}{3}, \frac{2l}{3}]$, the correction term is $q\frac{1-\phi 1(\beta x)}{k} + P1\frac{\phi 4[\beta(x-\frac{l}{3})]}{EI\beta^3}$

When $x \in (\frac{2l}{3}, l]$, the correction term is $q\frac{1-\phi 1(\beta x)}{k} + P1\frac{\phi 4[\beta(x-\frac{l}{3})]}{EI\beta^3} + P2\frac{\phi 4[\beta(x-\frac{2l}{3})]}{EI\beta^3}$

From the left end being the fixed end we know that $y0 = 0, \theta 0 = 0$, then the foundation beam deflection y can be written as

When

$$x \in [0, \frac{l}{3}],\ y = -M0\frac{\phi 3(\beta x)}{EI\beta^2} - Q0\frac{\phi 4(\beta x)}{EI\beta^3} + q\frac{1-\phi 1(\beta x)}{k} \tag{3}$$

When

$$x \in (\frac{l}{3}, \frac{2l}{3}],\ y = -M0\frac{\phi 3(\beta x)}{EI\beta^2} - Q0\frac{\phi 4(\beta x)}{EI\beta^3} + q\frac{1-\phi 1(\beta x)}{k} + P1\frac{\phi 4[\beta(x-\frac{l}{3})]}{EI\beta^3} \tag{4}$$

When

$$x \in (\frac{2l}{3}, l],\ y = -M0\frac{\phi 3(\beta x)}{EI\beta^2} - Q0\frac{\phi 4(\beta x)}{EI\beta^3} + q\frac{1-\phi 1(\beta x)}{k} + P1\frac{\phi 4[\beta(x-\frac{l}{3})]}{EI\beta^3} + P2\frac{\phi 4[\beta(x-\frac{2l}{3})]}{EI\beta^3} \tag{5}$$

When $x = l$, the bending moment M and shear force Q are expressed by the initial parameter method as

$$M = -EI\frac{d^2y}{dx^2} = M0\phi 1(\beta x) + \frac{Q0}{\beta}\phi 2(\beta x) - 4EI\beta^2 q\frac{\phi 3(\beta x)}{k} + \frac{P1}{\beta}\phi 2[\beta(x-\frac{l}{3})] + \frac{P2}{\beta}\phi 2[\beta(x-\frac{2l}{3})] \tag{6}$$

$$Q = \frac{dM}{dx} = -4\beta M0\phi 4(\beta x) + Q0\phi 1(\beta x) - 4EI\beta^3 q\frac{\phi 2(\beta x)}{k} + P1\phi 1[\beta(x-\frac{l}{3})] + P2\phi 1[\beta(x-\frac{2l}{3})] \tag{7}$$

The right end of the board is the free end, then when $x = l, M = Q = 0$, the formula (6), (7) joint solution to obtain.

$$M0 = \frac{\lambda 2[ch\beta l\sin\beta l + sh\beta l\cos\beta l] - 2\lambda 1 ch\beta l\cos\beta l}{\beta[(ch\beta l\sin\beta l)^2 - (sh\beta l\cos\beta l)^2] - 2\beta(ch\beta l\cos\beta l)^2} \tag{8}$$

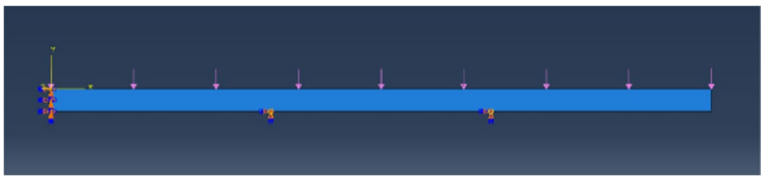

Fig. 5 Numerical simulation effect

Table 1 Model-related parameters

Parameter	Numerical value	Parameter	Numerical value
Modulus of elasticity of slab/(kPa)	3×10^7	Load / (kN·m^{-1})	50
Length of slab /m	9	Poisson's ratio of slab	0.2
Width of slab /m	0.3		

$$Q0=\frac{\lambda 2ch\beta l\cos\beta l+\lambda 1[ch\beta l\sin\beta l-sh\beta l\cos\beta l]}{\frac{1}{2}[(sh\beta l\cos\beta l)^2-(ch\beta l\sin\beta l)^2]-(ch\beta l\cos\beta l)^2} \tag{9}$$

$$\lambda 1=-2EI\beta^3 q\frac{sh\beta l\sin\beta l}{k}+\frac{P1}{2}(ch\frac{2}{3}\beta l\sin\frac{2}{3}\beta l+sh\frac{2}{3}\beta l\cos\frac{2}{3}\beta l)$$

ofwhich$+\frac{P1}{2}(ch\frac{1}{3}\beta l\sin\frac{1}{3}\beta l+sh\frac{1}{3}\beta l\cos\frac{1}{3}\beta l)$

$$\lambda 2=-2EI\beta^3 q\frac{ch\beta l\sin\beta l+sh\beta l\cos\beta l}{k}+P1ch\frac{2}{3}\beta l\cos\frac{2}{3}\beta l+P2ch\frac{1}{3}\beta l\cos\frac{1}{3}\beta l$$

The final settlement Table 2 and settlement diagram 6 are obtained by substituting Eqs. (8) and (9) into Eqs. (3), (4) and (5).

4 Numerical simulation of the corresponding analytical solution

Since the device is a dynamic problem during operation, accompanied by related processes such as circuit switching, casing expansion and contraction and dynamic balancing, it is impossible to solve its deflection deformation equation directly correspondingly, so the hitch plate is simplified to a beam structure with fixed left end and free right end, and the two adaptive devices are simplified to hinge supports. The beam is subjected to a uniform load above, as shown in Fig. 5.

With reference to actual engineering and relevant literature, the model parameters are shown in Table 1.

The analytical and numerical solution deflections and the errors between the two are shown in Table 2 and Fig. 6.

The following comparison graphs were drawn from Table 2.

As seen in Table 2 and Fig. 6.

(1). The analytical solution deflection tends to rise steadily, reaching a maximum settlement of 2.571 cm at the end of the hitching slab; the numerical solution deflection tends to zero at 3 m and 6 m respectively, i.e. at the adaptive device, and there is a back-arch phenomenon within 3-6 m, with a maximum bulge of

Table 2 Comparison of analytical and numerical solutions for slap settlement data

Distance from fixed end /m	Analytical solution of settlement /cm	Numerical solution settlement /cm	Error /cm
0	0	0	0
0.5	0.007	0.013	-0.006
1.0	0.012	0.033	-0.021
1.5	0.035	0.044	-0.009
2.0	0.051	0.043	0.008
2.5	0.094	0.021	0.073
3.0	0.131	0.004	0.127
3.5	0.193	-0.019	0.212
4.0	0.277	-0.051	0.328
4.5	0.361	-0.089	0.450
5.0	0.484	-0.103	0.587
5.5	0.623	-0.086	0.709
6.0	0.793	0.011	0.782
6.5	0.998	0.219	0.779
7.0	1.225	0.552	0.673
7.5	1.517	0.936	0.581
8.0	1.813	1.368	0.445
8.5	2.175	1.811	0.364
9.0	2.571	2.263	0.308

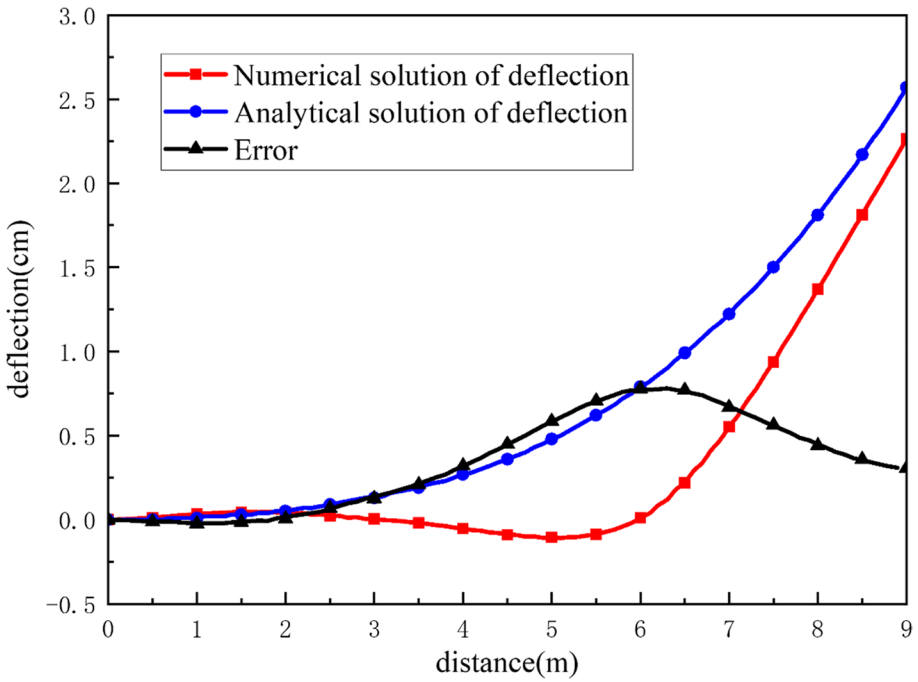

Fig. 6 Analytical solution, numerical solution and error diagram

0.103 cm, and the deflection rises steadily from 6-9 m, reaching a maximum settlement of 2.263 cm at the end of the hitching slab. The presence of the reverse arch is due to the fact that the numerical solution model only receives the upper

uniform load and the vertical support below, whereas the analytical solution equation takes into account the support reaction of the soil under the action of the slap in advance, which results in a smoother curve.

(2). The rate of change of the longitudinal slope of the analytical and numerical solutions is 2.8‰ and 2.5‰ respectively, which meets《Code for design of urban road engineering》. The error between the two gradually increases within 0-6 m, with a maximum error of 0.782 cm, and gradually decreases within 6-9 m, to 0.308 cm at the free end. 12.0% error between the two at the end of the hitch can be used as theoretical support to prove the feasibility of the adaptive device.

5 Experimental validation

To verify the feasibility of the adaptive device, it was applied to the Jingzhou City Xingang Avenue span bridge project. The bridge has a total length of 389 m, and the span combination is $4\times30+35+45+35+3\times30+2\times32$ m. The left and right widths are both 13.3 m, as shown in Fig. 7.

Jingzhou West Ring Road Crossing Bridge Project is located in Jianghan Plain, the foundation soil is mainly powder clay, chalk and silt, which is prone to uneven settlement and causes the problem of jumping traffic at the bridge head. The project adopts adaptive device to solve the problem of jumping traffic at the bridge head, the length of the lap is 9 m, one end is cemented on the bridge deck, the other end is used as the free end, and the mat is laid under the free end to reduce the later settlement of the soil layer under the slap.

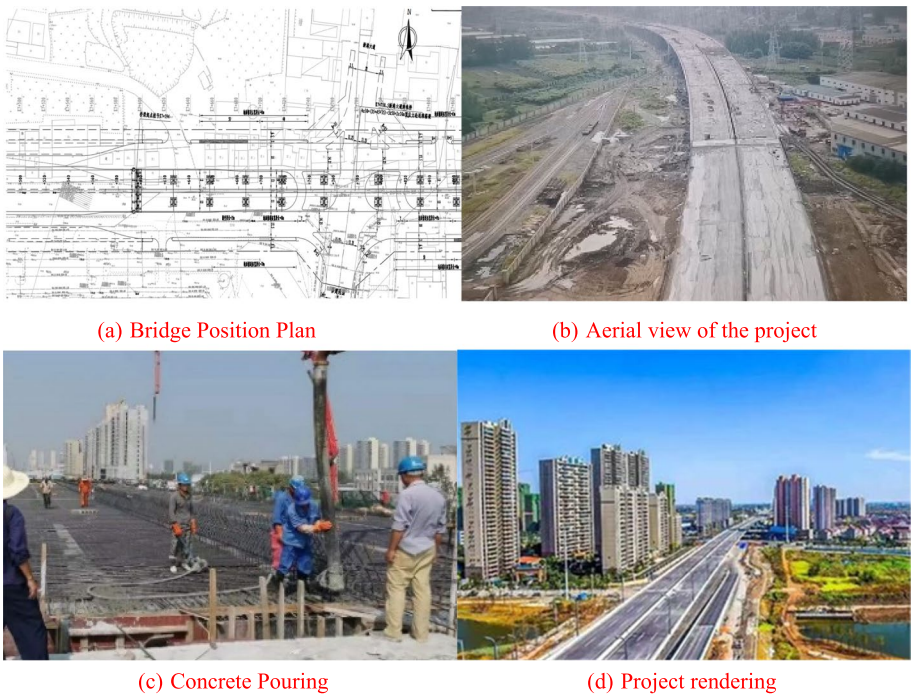

Fig. 7 Jingzhou Xingang Avenue cross-line bridge project

For the convenience of differentiation, the device near the fixed end is device No. 1, and the device near the free end is device No. 2. The lifting length of the two adaptive devices and the settlement at the end of the slap are observed once every 20 days after the construction is completed, as shown in Table 3.

The following comparison curves are plotted according to Table 3.

As seen from Table 3 and Fig. 8.

(1). The trend of the three curves is roughly the same, all of them are from 0 at the beginning, smoothly increasing to the maximum value after 360 days, with smooth slope and no sudden change.

(2). The elongation of No.1 device is larger than No.2 device until 180 days, which means that in the first half of dynamic adjustment, No.1 device near the fixed end dominates and shares most of the settlement of the hitch under the load; after 180 days, the elongation of No.2 hitch near the free end exceeds that of No.1 hitch, which means that in the second half of dynamic adjustment, the settlement of the hitch near the free end is larger and the distance to be lifted is higher. The adaptive devices No. 1 and No. 2 reached the maximum values of the corresponding elongations of 1.63 cm and 1.97 cm, respectively, at 360 days.

(3). Settlement at the end of the hitch gradually becomes larger with time, and the slope of the curve gradually becomes smaller and tends to be stable after 300 days. The final settlement at the end of the slab is 3.74 cm, and the longitudinal slope change rate is 4.15‰, which meets 《Code for design of urban road engineering》.

Table 3 Device lifting distance and slap settlement table

Putting into use time /d	Lifting distance of No.1 device /cm	Lifting distance of No.2 device /cm	Settlement value at the end of the slab /cm
0	0	0	0
20	0.03	0.02	0.08
40	0.08	0.06	0.19
60	0.15	0.10	0.35
80	0.25	0.17	0.50
100	0.36	0.23	0.69
120	0.50	0.31	0.88
140	0.71	0.45	1.07
160	0.91	0.69	1.29
180	1.07	0.96	1.51
200	1.17	1.19	1.77
220	1.27	1.37	2.10
240	1.36	1.50	2.39
260	1.43	1.65	2.68
280	1.51	1.77	2.95
300	1.57	1.85	3.25
320	1.61	1.89	3.49
340	1.62	1.95	3.64
360	1.63	1.97	3.74

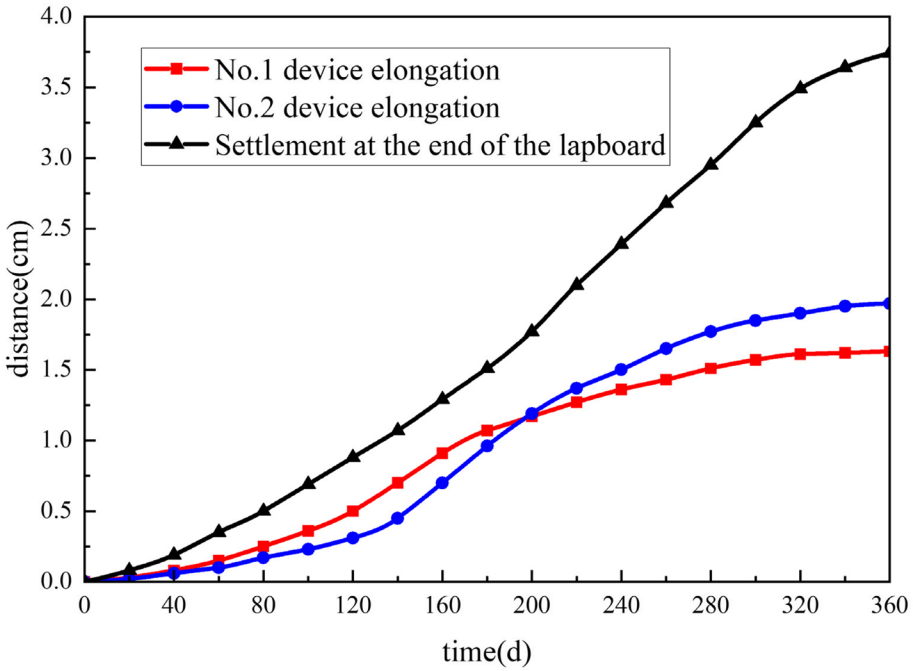

Fig. 8 Device lifting distance and slap settlement diagram

6 Conclusion

In this study, a new adaptive device was proposed, the analytical solution of the deflection of the slap under the device was calculated, the finite element simulation process under the corresponding mechanical model was constructed, and the adaptive device to the actual project was applied. The main research findings are as follows.

(1). The new adaptive device can realize self-adjustment thus avoiding the phenomenon of jumping at the bridge head by setting the first hitch plate, the second hitch plate, the pile base, the hydraulic device, the mirror-reflective photoelectric switch, the horizontal switch and the contact switch in the case of soil foundation settlement, overall settlement and hitch plate tilt.

(2). The maximum deflection of the analytical and numerical solutions of the hitch under the adaptive device is 2.571 cm and 2.263 cm, and the corresponding longitudinal slope change rate is 2.8‰ and 2.5‰, which conforms to the corresponding specification.

(3). In the actual project, the lifting distance of certain devices and the settlement value of the end of the hitching slab were measured every 20 days reached the maximum value of 3.74 cm. Both theory and practice show that the adaptive device can effectively alleviate the uneven settlement and eliminate the height difference of the transition section of the road and bridge, which provides a reference for solving the problem of jumping traffic at the bridge head in the actual project.

Acknowledgements
Not applicable.

Authors' contributions
Bingliang Cai: Writing original draft, Formal analysis, Experiment. Deyi Chen: Project administration, Review. Shiping Huang: Data processing. All authors read and approved the final manuscript.

Funding
This study is supported by the Project of National Natural Science Foundation (No. 11672108) and Research Project of Hubei Provincial Department of Education (No. Q20221305).

Availability of data and materials
Supplementary data to this article can be received from the corresponding author on reasonable request.

Declarations

Competing interests
The authors declare that there is no conflict of interest regarding the publication of this paper.

Received: 12 April 2023 Accepted: 30 June 2023
Published online: 28 July 2023

References

Bai XH, Huang XZ, Zhang W (2013) Bearing capacity of square footing supported by a geobelt-reinforced crushed stone cushion on soft soil. Geotext Geomembr 38:37–42
Bao C, Xu F, Chen G et al (2019) Seismic vulnerability analysis of structure subjected to uneven foundation settlement. Appl Sci 9(17):3507
Briaud JL, Lim Y (1997) Soil-nailed wall under piled bridge abutment: simulation and guidelines. J Geotech Geoenvironmental Eng 123(11):1043–1050
Chakraborty M, Kumar J (2014) Bearing capacity of circular foundations reinforced with geogrid sheets. Soils Found 54(4):820–832
Chen QM, Abu-Farsakh M (2015) Ultimate bearing capacity analysis of strip footings on reinforced soil foundation. Soils Found 55(1):74–85
Chen QM, Abu-Farsakh M (2016) Mitigating the bridge end bump problem: a case study of a new approach slab system with geosynthetic reinforced soil foundation. Geotext Geomembr 44(1):39–50
Chen QM, Abu-Farsakh M, Sharma R (2009) Experimental and analytical studies of reinforced crushed limestone. Geotext Geomembr 27(5):357–367
Demir A, Laman M, Yildiz A et al (2013) Large scale field tests on geogrid-reinforced granular fill underlain by clay soil. Geotext Geomembr 38:1–15
Jawad S, Han J, Abdulrasool G et al (2021) Responses of single and group piles within MSE walls under static and cyclic lateral loads. Geotext Geomembr 49(4):1019–1035
Kim W, Laman JA (2012) Seven-year field monitoring of four integral abutment bridges. J Perform Constr Facil 26(1):54–64
Lin KQ, Wong IH (1999) Use of deep cement mixing to reduce settlements at bridge approaches. J Geotech Geoenvironmental Eng 125(4):309–320
Liu H, Han J, Parsons RL (2021) Mitigation of seasonal temperature change-induced problems with integral bridge abutments using EPS foam and geogrid. Geotext Geomembr 49(5):1380–1392
Liu H, Han J, Jawad S et al (2022) Effects of traffic loading on seasonal temperature change-induced problems for integral bridge approaches and mitigation with geosynthetic reinforcement. Int J Geomech 22(6):04022082
Long JH, Olson SM, Stark TD et al (1998) Differential movement at embankment-bridge structure interface in Illinois. Transp Res Rec 1633(1):53–60
Miao L, Wang F, Han J et al (2014) Benefits of geosynthetic reinforcement in widening of embankments subjected to foundation differential settlement. Geosynth Int 21(5):321–332
Naeini SA, Gholampoor N (2014) Cyclic behaviour of dry silty sand reinforced with a geotextile. Geotext Geomembr 42(6):611–619
Sharma R, Chen Q, Abu-Farsakh M et al (2009) Analytical modeling of geogrid reinforced soil foundation. Geotext Geomembr 27(1):63–72
Tatsuoka F, Hirakawa D, Nojiri M et al (2009) A new type of integral bridge comprising geosynthetic-reinforced soil walls. Geosynth Int 16(4):301–326
Wang CD, Zhou S, Wang B et al (2015) Differential settlements in foundations under embankment load: theoretical model and experimental verification. Geomech Eng 8(2):283–303
Wong HKW (1994) Effect of orientation of approach slabs on pavement deformation. J Transp Eng 120(4):590–602
Xiao C, Han J, Zhang Z (2016) Experimental study on performance of geosynthetic-reinforced soil model walls on rigid foundations subjected to static footing loading. Geotext Geomembr 44(1):81–94
Yasrobi SY, Ng KW, Edgar TV et al (2016) Investigation of approach slab settlement for highway infrastructure. Transp Geotech 6:1–15

Publisher's Note